Available online at www.sciencedirect.com

ScienceDirect

Procedia Structural Integrity 2 (2016) 2734–2741

Structural Integrity Procedia

www.elsevier.com/locate/procedia

21st European Conference on Fracture, ECF21, 20-24 June 2016, Catania, Italy

Fatigue crack growth in round bars for rock anchorages: the role of residual stresses

Jesús Toribio*, Juan-Carlos Matos, Beatriz González, José Escuadra

Fracture and Structural Integrity Research Group, University of Salamanca, E.P.S., Campus Viriato, Avda. Requejo 33, 49022 Zamora, Spain

Abstract

The role of different residual stress profiles in the fatigue crack growth is studied in prestressing steel wires under tension loading or bending moment. The crack front evolution is analyzed by means of a computer program on the basis of the Walker law. Numerical results indicate that the absence of residual stresses makes the crack propagate following a preferential cracking path. When surface residual stresses are tensile and, correspondingly, core residual stresses are compressive, the fatigue crack fronts rapidly converge towards a quasi-straight shape. When surface residual stresses are compressive, with their corresponding tensile stresses in the core area, a preferential cracking path also appears.

Keywords: Round bars; semi-elliptical surface cracks; numerical modelling; Walker law; residual stress profile; fatigue crack propagation

1. Introduction

High-strength cold-drawn prestressing steel wires, frequently used as components of anchorage in rocks, are manufactured from hot rolled pearlitic steel bars and have excellent mechanical properties. As studied by Toribio and Valiente (2004), the cold drawing process improves the mechanical properties of the material by increasing the yield strength, the ultimate tensile strength (UTS), the fracture toughness, etc. Elices (2004) showed that such a manufacturing technique induces strong tensile residual stresses at the wire surface and compressive ones in the core. In the papers by He et al. (2003) and Atienza et al. (2005), it is shown that the residual stress distribution in cold drawn wires can be evaluated by experimental methods (e.g., neutron and X-ray diffraction techniques) and by numerical procedures such as the finite element method (FEM). In the work by Atienza et al. (2005), the isotropic von Mises

* Corresponding author. Tel.: +34-980-545000; fax: +34-980-545002.
E-mail address: toribio@usal.es

10.1016/j.prostr.2016.06.341

yield criterion is used to analyze the distribution of residual stresses in the wire, as well as in the more recent paper by Toribio et al. (2015), whereas He et al. (2003) employed a texture-based anisotropic yield locus in the FEM computations. The analysis by Martínez-Pérez et al. (2004) deals with the roles of the two micro-constituents of pearlite, ferrite and cementite, showing that both exhibit different residual stress profiles.

Toribio et al. (2015) demonstrated that the use of a varying die angle during cold drawing can modify the resulting residual stress profile. Atienza and Elices (2003) showed that the distribution of residual stresses can affect the mechanical properties obtained through a standard tension test. Zeren and Zeren (2003) concluded that residual stresses can also affect the phenomenon of stress relaxation in such materials. In prestressing steel wires subjected to tensile cyclic loading, after-drawing residual stresses affect the crack front shape in such a manner that it creates the so-called *gull effect* described by Toribio et al. (2010), it consisting of retardation of fatigue crack growth in the areas of compressive residual stresses and acceleration in the tensile areas. In agreement with this idea, the studies by Toyosada et al. (1997) indicate that, under cyclic loading, tensile residual stresses create only a slight increase in crack propagation rate and compressive residual stresses create a big decrease in crack propagation rate.

This paper analyzes the influence of different residual stress distributions (of both tensile and compressive nature) on the fatigue crack propagation in high-strength cold-drawn prestressing steel wires, comparing the results with those associated with a material free of residual stresses.

Nomenclature

a	crack depth
a/b	crack aspect ratio
a/D	relative crack depth
$\Delta a(i)$	crack advance at the point i in a given iteration
$\Delta a\{\max\}$	maximum value of $\Delta a(i)$ over the crack front
b	second dimension of the crack (modeled as a semiellipse)
C	Paris constant
$\mathrm{d}a/\mathrm{d}N$	crack growth rate
D	diameter of wire
F	tensile load
K	stress intensity factor
$K_{\max}$	maximum stress intensity factor (during fatigue)
$K_{\max}(i)$	maximum stress intensity factor at the point i in a given iteration
$K_{\max}\{\max\}$	maximum value of $K_{\max}(i)$ over the crack front
m	Paris exponent
M	bending moment
r	radial coordinate
R	ratio of the minimum to the maximum stress
RS0	residual stress profile 0 (material free of residual stresses)
RS1	residual stress profile 1 (tensile residual stresses at surface)
RS2	residual stress profile 2 (compressive residual stresses at surface)
$\sigma_{\mathrm{app,max}}$	maximum applied remote stresses
σ_{res}	residual stresses (in axial direction)

2. Numerical method

In this work, a geometrical model consisting on a round bar was used (it representing a cold drawn prestressing steel wire) with a transverse surface crack, subjected to tension or bending (Fig. 1). The material model was a typical high-strength steel characterized by a Paris exponent m = 3, with R-ratio = 0, taken from the experiments performed by Toribio et al. (2009). Two profiles of residual stress in axial direction (σ_{res}) were used in the computations satisfying the global equilibrium conditions over the transverse section of a wire.

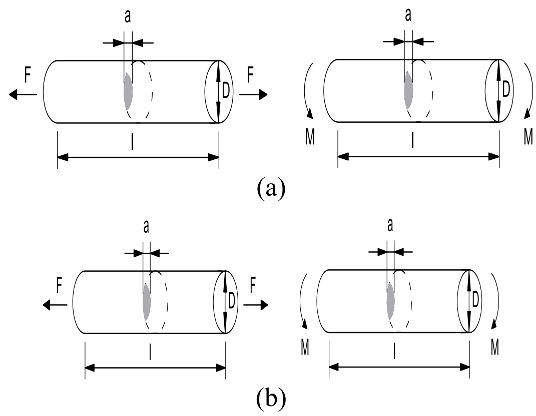

Fig. 1. Cracked bar under: (a) tension loading; (b) bending moment.

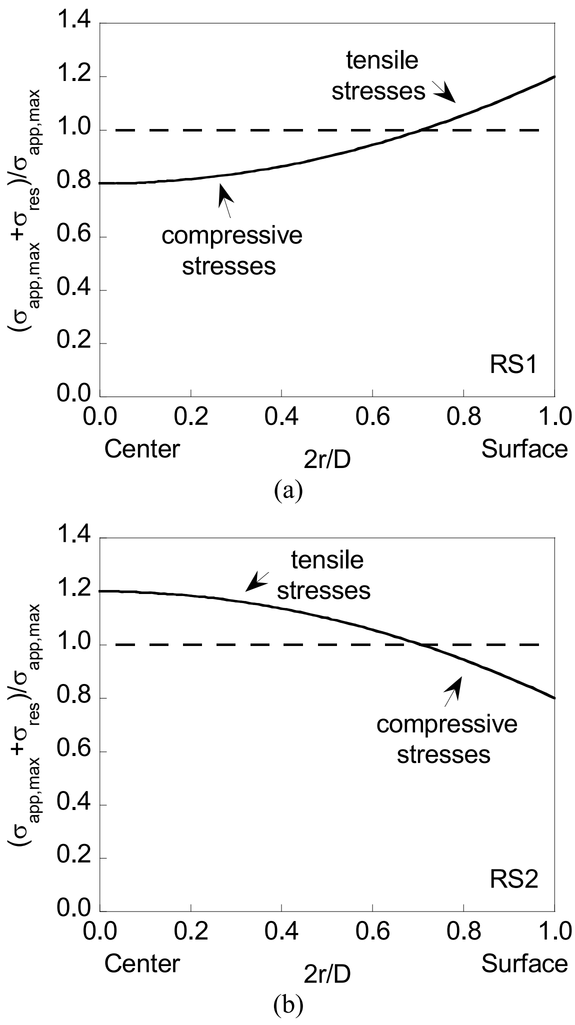

Fig. 2. Residual stress profile in cold drawn wires: (a) RS1; (b) RS2.

Fig. 2 shows the dimensionless stress profile $(\sigma_{app,max}+\sigma_{res})/\sigma_{app,max}$ as a function of the dimensionless ratio $2r/D$ (where $\sigma_{app,max}$ is the maximum applied remote stress, r the radial coordinate and D the diameter of wire). Residual stress profile 1 (RS1) presents compressive stresses in the center area and tensile stresses near the surface (Fig. 2a). On the other hand, residual stress profile 2 (RS2) exhibits tensions in the core zone and compressions in the near-surface area (Fig. 2b). For comparison purposes, residual stress profile 0 (RS0) is that representing a material free of residual stresses over the whole area.

The analyses of this paper are based on the fatigue crack growth equation proposed by Walker (1970), usually known as Walker law (used to model the crack advance under cyclic loading):

$$\frac{\mathrm{d}a}{\mathrm{d}N} = C\left(K_{\max}\right)^{\mathrm{m}} \tag{1}$$

where the Walker exponent was supposed to be zero (on assuming that the R-ratio is always lower than zero), K_{max} is the maximum stress intensity factor (SIF K) during fatigue, and C and m are the Paris coefficients for R-ratio = 0. The SIF expression proposed by Shin and Cai (2004) was used throughout this paper. On the basis of this K-solution and using the superposition principle, the value of K_{max} can be obtained.

The crack front was characterized as an ellipse of semiaxes a (crack depth) and b (second geometric parameter of the crack) as shown in Fig. 3. It was discretized as a set of points (obtained by dividing the ellipse in parts of equal length applying the Simpson rule). The advance at each point of the crack (i) is perpendicular to the crack front. The point at the crack front associated with the maximum value of K_{max}, $(K_{max})\{\max\}$, is advanced a fixed value $\Delta a\{\max\}$ and the rest of the points considering the Walker law as follows:

$$\Delta a(i) = \Delta a\{\max\}\left[\frac{K_{\max}(i)}{(K_{\max})\{\max\}}\right]^{\mathrm{m}} \tag{2}$$

Following this procedure, one obtains a set of new points representing the advanced crack, so that a new ellipse can be fitted. The process is repeated up to reaching the desired crack length.

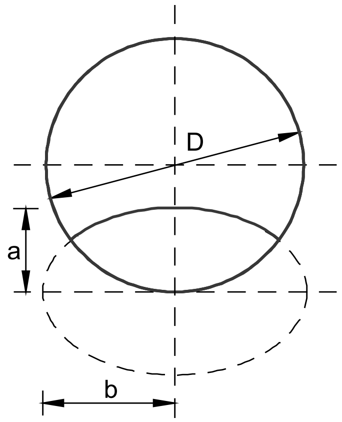

Fig. 3. Surface crack with semi-elliptical shape.

3. Numerical results

Figs. 4 and 5 show the evolution of the crack front during fatigue crack propagation from different initial geometries: relative crack depths a/D = {0.1, 0.2, 0.3, 0.4, 0.5, 0.6, 0.7} and crack aspect ratios a/b = 1 (semi-circular front) and a/b = 0.1 (quasi-straight front). Fig. 4 shows the particular results for tension loading whereas Fig. 5 does the same for bending moment.

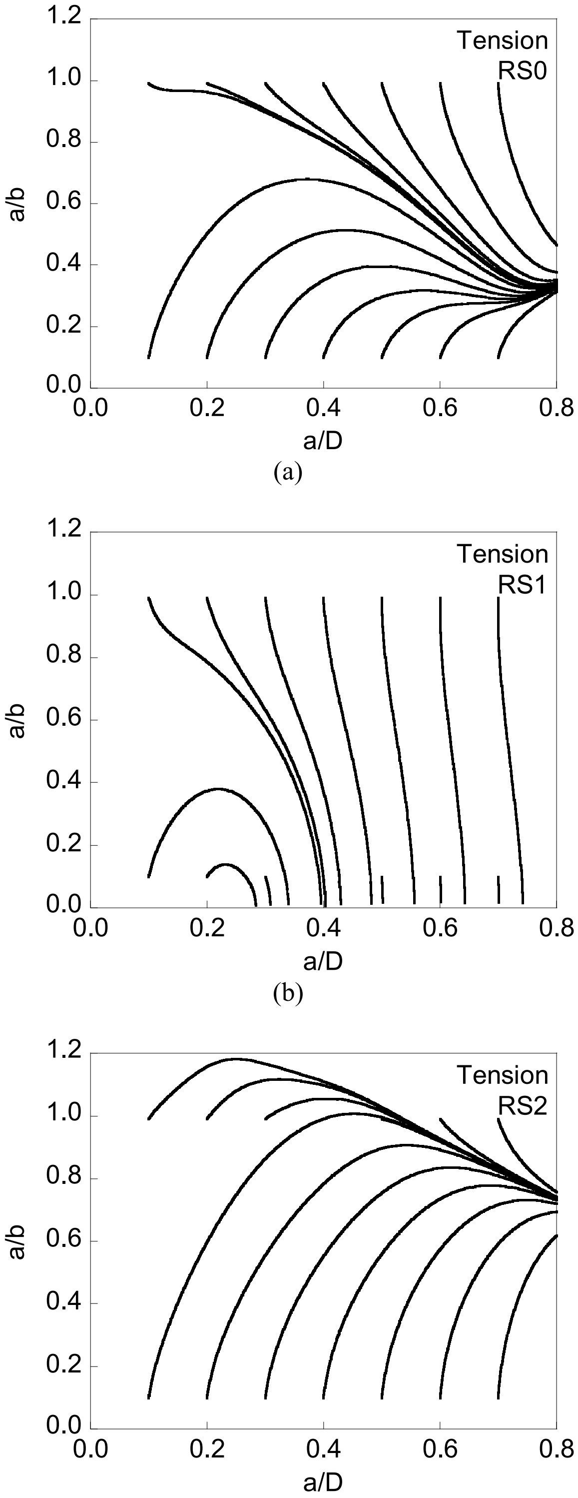

(a)

(b)

(c)

Fig. 4. Crack aspect ratio *a*/*b* *versus* relative crack depth *a*/*D* for tension loading: (a) RS0; (b) RS1; (c) RS2.

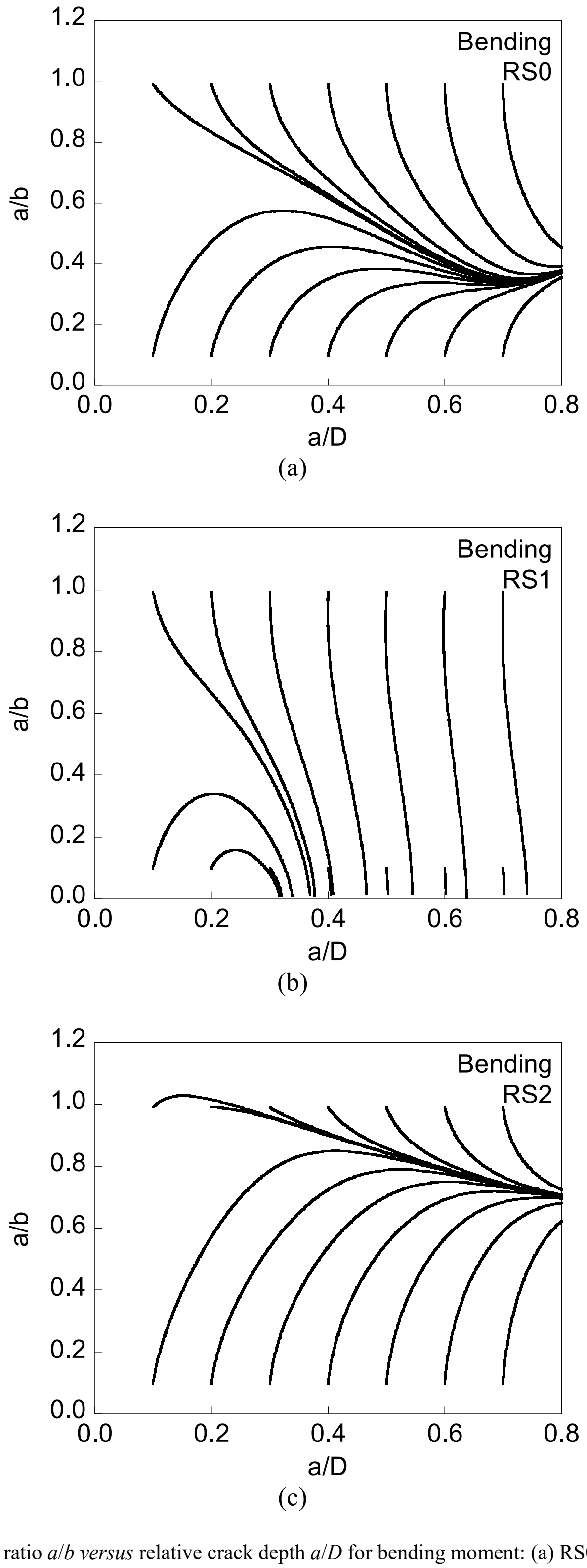

Fig. 5. Crack aspect ratio *a*/*b versus* relative crack depth *a*/*D* for bending moment: (a) RS0; (b) RS1; (c) RS2.

In the case of zero residual stresses (RS0) the crack tends to growth by adopting a sort of preferential cracking path, this result being consistent with that obtained by Toribio et al. (2012) for both fatigue in air and corrosion-fatigue. In a plot a/b-a/D, the afore-said path is higher (greater a/b for a given a/D) in tension (Fig. 4a) than in bending (Fig. 5a).

A residual stress profile with tensions in the vicinity of the wire surface and compressions in the central area RS1 makes the crack propagate towards a quasi-straight crack front. Such a profile seems to affect crack propagation both in tension (Fig. 4b) and in bending (Fig. 5b).

A residual stress profile with compressions in the vicinity of the wire surface and tensions in the central area RS2 makes the crack propagate towards a preferential crack path (as in the case of material free of residual stresses). In a plot a/b-a/D, such a path is higher (greater a/b for a given a/D) in tension (Fig. 4c) than in bending (Fig. 5c), and higher than in the absence of any residual stresses (Figs. 4a and 5a).

4. Conclusions

On the basis of the numerical results, the following conclusions can be drawn:

(i) Compressive residual stresses induce fatigue crack growth retardation, while tensile ones accelerate cracking, thereby modifying the crack aspect ratio.

(ii) When the compressions are located near the surface and the tensions in the central area, the consequence is the crack advance towards higher aspect ratios.

(iii) When the situation is the opposite (tensions near the surface and compressions at the centre) then the aspect ratio decreases, very quickly, during crack advance.

Acknowledgements

The authors wish to acknowledge the financial support provided by the following Spanish Institutions: Ministry for Science and Technology (MICYT; Grant MAT2002-01831), Ministry for Education and Science (MEC; Grant BIA2005-08965), Ministry for Science and Innovation (MICINN; Grant BIA2008-06810), Ministry for Economy and Competitiveness (MINECO; Grant BIA2011-27870), Junta de Castilla y León (JCyL; Grants SA067A05, SA111A07 and SA039A08) and the Spanish University Foundation "Memoria de D. Samuel Solórzano Barruso" (Grant 2016/00017/001).

References

Atienza, J.M., Elices, M., 2003. Influence of Residual Stresses in the Tensile Test of Cold Drawn Wires. Materials and Structures 36, 548–552.

Atienza, J.M., Martínez-Pérez, M.L., Ruiz-Hervias, J., Mompean, F., García-Hernández, M., Elices, M., 2005. Residual Stresses in Cold Drawn Ferritic Rods. Scripta Materialia 52, 305–309.

Elices, M., 2004. Influence of Residual Stresses in the Performance of Cold-Drawn Pearlitic Wires. Journal of Materials Science 39, 3889–3899.

He, S., Van Bael, A., Li, S.Y., Van Houtte, P., Mei, F., Sarban, A., 2003. Residual Stress Determination in Cold Drawn Steel Wire by FEM Simulation and X-Ray Diffraction. Materials Science and Engineering A 346, 101–107.

Martínez-Pérez, M.L., Mompean, F.J., Ruiz-Hervias, J., Borlado, C.R., Atienza, J.M., García-Hernández, M., Elices, M., Gil-Sevillano, J., Peng, R.L., Buslaps, T., 2004. Residual Stress Profiling in the Ferrite and Cementite Phases of Cold-Drawn Steel Rods by Synchrotron X-Ray and Neutron Diffraction. Acta Materialia 52, 5303–5313.

Shin, C.S., Cai, C.Q., 2004. Experimental and Finite Element Analyses on Stress Intensity Factors of Elliptical Surface Crack in a Circular Shaft under Tension and Bending. International Journal of Fracture 129, 239–264.

Toribio, J., González, B., Matos, J.C., 2010. Fatigue and Fracture Paths in Cold Drawn Pearlitic Steel. Engineering Fracture Mechanics 77, 2024–2032.

Toribio, J., Lorenzo, M., Vergara, D., 2015. On the Use of Varying Die Angle for Improving the Resistance to Hydrogen Embrittlement of Cold Drawn Prestressing Steel Wires. Engineering Failure Analysis 47, 273–282.

Toribio, J., Matos, J.C., González, B., 2009. Micro- and Macro-Approach to the Fatigue Crack Growth in Progressively Drawn Pearlitic Steels at Different *R*-Ratios. International Journal of Fatigue 31, 2014–2021.

Toribio, J., Matos, J.C., González, B., Escuadra, J., 2012. Environmentally-Assisted Fatigue Crack Growth in Prestressing Steel Wires. Materials Science 47, 764–772.

Toribio, J., Valiente, A., 2004. Approximate Evaluation of Directional Toughness in Heavily Drawn Pearlitic Steels. Materials Letters 58, 3514–3517.

Toyosada, M., Niwa, T., Sakai, J., 1997. Physical Meaning of ΔK_{RP} and Fatigue Crack Propagation in the Residual Stress Distribution Field. International Journal of Fatigue 19, 161–166.

Walker, K., 1970. The Effect of Stress Ratio During Crack Propagation and Fatigue for 2024-T3 and 7075-T6 Aluminum, in "Effects of Environment and Complex Load History on Fatigue Life (ASTM STP 462)". In: ASTM International, Philadelphia, pp. 1.

Zeren, A., Zeren, M., 2003. Stress Relaxation Properties of Prestressed Steel Wires. Journal of Materials Processing Technology 141, 86–92.